Detector Requirements and Experimental Conditions at CLIC

André Sailer
on behalf of the CLICdp collaboration

CERN-EP-LCD

CLICdp Advisory Board
April 17–18, 2018

Table of Contents

Section 1:

Luminosity and Beam-Beam Effects

- Large luminosities require high bunch charge N and small beams $\sigma_{x/y/z}$ (given the other constraints from the accelerator) $L \propto \frac{N^2}{\sigma_x \sigma_y}$
- Leads to large electromagnetic fields during bunch crossing $B \propto \frac{\gamma N}{\sigma_z(\sigma_x+\sigma_y)}$
  - Use flat beams $\sigma_y \ll \sigma_x$
- The bunch particles are strongly deflected by the fields and radiate *Beamstrahlung*

Start

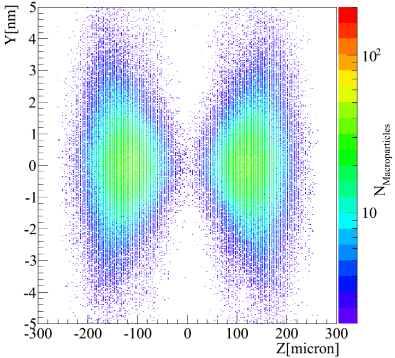

N.b.: Factor 1000 between Y and Z!
Animated bunch crossing

- *Beamstrahlung* radiation leads to collisions far below the nominal centre-of-mass energy $\sqrt{s}$
  - Large fraction at nominal $\sqrt{s}$
- **Luminosity spectrum $\mathcal{L}(E_1, E_2)$**
- Collisions between $e^{\pm}\gamma$ and $\gamma\gamma$

Luminosity in $10^{34}\mathrm{cm}^{-2}\mathrm{s}^{-1}$

Collision	380 GeV	3 TeV
e^-e^+	1.51	6.35
$e^-\gamma$	0.80	5.05
γe^+	0.80	5.05
$\gamma\gamma$	0.50	4.49

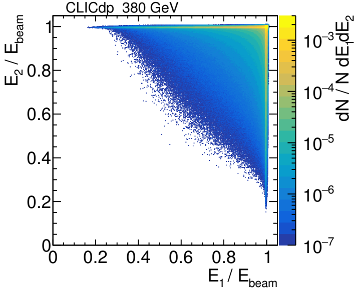

$\sqrt{s'}/\sqrt{s}$	380 GeV	3 TeV
> 0.99	58%	36%
> 0.90	87%	57%
> 0.80	96%	69%
> 0.70	98.7%	76.8%
> 0.50	99.96%	88.6%

Beamstrahlung and Luminosity

- *Beamstrahlung* radiation leads to collisions far below the nominal centre-of-mass energy $\sqrt{s}$
  - Large fraction at nominal $\sqrt{s}$
- **Luminosity spectrum $\mathcal{L}(E_1, E_2)$**
- Collisions between $e^{\pm}\gamma$ and $\gamma\gamma$

Luminosity in $10^{34}\mathrm{cm}^{-2}\mathrm{s}^{-1}$

Collision	380 GeV	3 TeV
e^-e^+	1.51	6.35
$e^-\gamma$	0.80	5.05
γe^+	0.80	5.05
$\gamma\gamma$	0.50	4.49

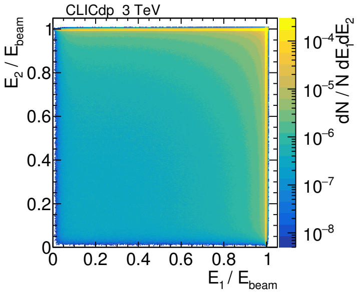

$\sqrt{s'}/\sqrt{s}$	380 GeV	3 TeV
> 0.99	58%	36%
> 0.90	87%	57%
> 0.80	96%	69%
> 0.70	98.7%	76.8%
> 0.50	99.96%	88.6%

Beamstrahlung and Luminosity

- *Beamstrahlung* radiation leads to collisions far below the nominal centre-of-mass energy $\sqrt{s}$
  - Large fraction at nominal $\sqrt{s}$
- Luminosity spectrum $\mathcal{L}(E_1, E_2)$
- **Collisions between $e^{\pm}\gamma$ and $\gamma\gamma$**

Luminosity in $10^{34}\mathrm{cm}^{-2}\mathrm{s}^{-1}$

Collision	380 GeV	3 TeV
e^-e^+	1.51	6.35
$e^-\gamma$	0.80	5.05
γe^+	0.80	5.05
$\gamma\gamma$	0.50	4.49

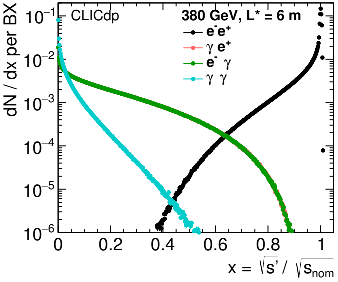

$\sqrt{s'}/\sqrt{s}$	380 GeV	3 TeV
> 0.99	58%	36%
> 0.90	87%	57%
> 0.80	96%	69%
> 0.70	98.7%	76.8%
> 0.50	99.96%	88.6%

Beamstrahlung and Luminosity

- *Beamstrahlung* radiation leads to collisions far below the nominal centre-of-mass energy $\sqrt{s}$
  - Large fraction at nominal $\sqrt{s}$
- Luminosity spectrum $\mathcal{L}(E_1, E_2)$
- **Collisions between $e^{\pm}$ γ and $\gamma\gamma$**

Luminosity in $10^{34}\mathrm{cm}^{-2}\mathrm{s}^{-1}$

Collision	380 GeV	3 TeV
e^-e^+	1.51	6.35
$e^-\gamma$	0.80	5.05
γe^+	0.80	5.05
$\gamma\gamma$	0.50	4.49

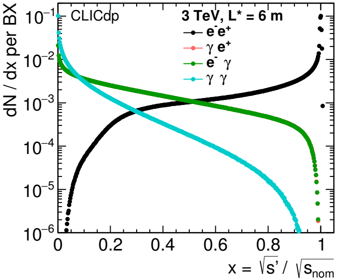

$\sqrt{s'}/\sqrt{s}$	380 GeV	3 TeV
> 0.99	58%	36%
> 0.90	87%	57%
> 0.80	96%	69%
> 0.70	98.7%	76.8%
> 0.50	99.96%	88.6%

Backgrounds I

- Beamstrahlung photons collide with beam particles or other photons

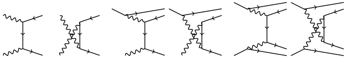

  - *Incoherent* e^+e^- pairs
  - $q\overline{q}$ pairs in $\gamma\gamma \to$ Hadron events
- Incoherent pairs have largest concentration at small angles
- backgrounds strongly depend on centre-of-mass energy

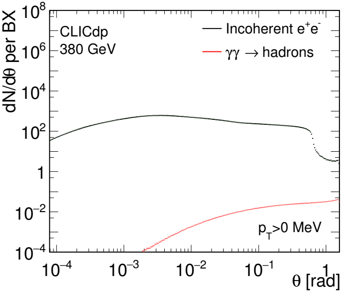

- Beamstrahlung photons collide with beam particles or other photons

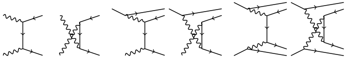

  - *Incoherent* e^+e^- pairs
  - $q\overline{q}$ pairs in $\gamma\gamma \rightarrow$ Hadron events
- Incoherent pairs have largest concentration at small angles
- backgrounds strongly depend on centre-of-mass energy

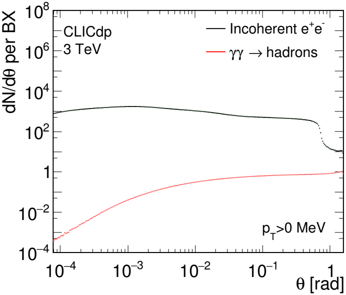

Backgrounds I

- Beamstrahlung photons collide with beam particles or other photons

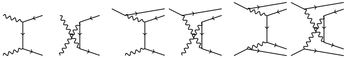

  - *Incoherent* e^+e^- pairs
  - $q\overline{q}$ pairs in $\gamma\gamma \rightarrow$ Hadron events
- Incoherent pairs have largest concentration at small angles
- backgrounds strongly depend on centre-of-mass energy

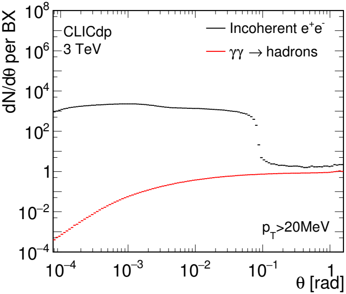

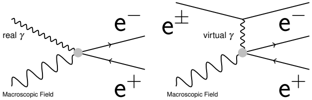

- Real or virtual photons interact with the very strong fields to create e^+e^- pairs
- Coherent processes only significant for $\sqrt{s} > 1$ TeV
- Coherent pairs limit the lower acceptance of the detector to 10 mrad around the outgoing beam-axis

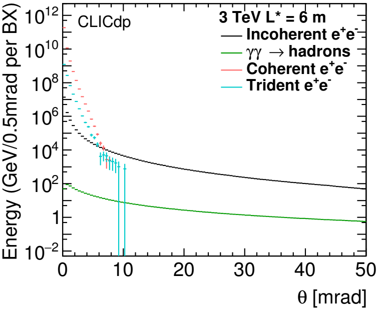

- Very large gradient and room temperature copper cavities require short RF pulses of less than 200 ns
- Bunch spacing of $\Delta t = 0.5$ ns with ≈ 300 bunches per train at 50 Hz
- Short bunch spacing requires crossing angle θ_c to avoid parasitic collision
- Crab crossing scheme to avoid loss of geometrical overlap of colliding bunches

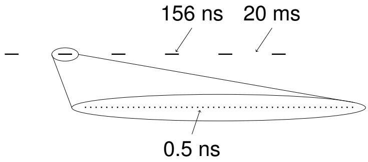

Par.	Unit	380 GeV	3 TeV
θ_c	mrad	16.5	20
n_b		352	312
N		$5.2 \cdot 10^9$	$3.72 \cdot 10^9$
σ_x	nm	≈ 149	≈ 45
σ_y	nm	≈ 2.9	≈ 1
σ_z	µm	70	44
$\mathcal{L}$	$1/\text{cm}^2\text{s}^1$	$1.5 \cdot 10^{34}$	$5.9 \cdot 10^{34}$
$\mathcal{L}_{0.01}$	$1/\text{cm}^2\text{s}^1$	$0.9 \cdot 10^{34}$	$2.0 \cdot 10^{34}$

Section 2:

Detector Requirements due to Beam and Backgrounds

- Vertex Detector
- Readout and Power Pulsing
- Very Forward Region
- Calorimeter Endcaps

Vertex Detector Radius

- Large flux of low momentum particles from incoherent pairs limits the inner radius of the vertex detector
- Solenoid field reduces radius of particles
- Smaller radius possible at lower centre-of-mass energy

Rate of incoherent pair particles close to the interaction point for 3 TeV

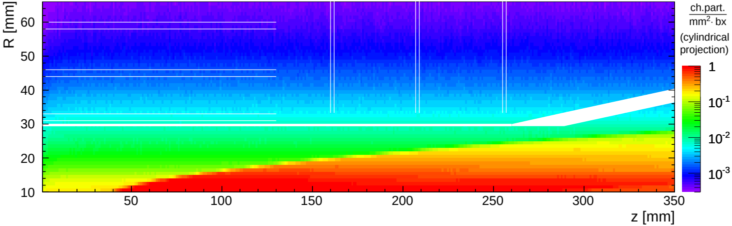

Full simulations to obtain occupancies of all tracking detectors have been studied for $\gamma\gamma \rightarrow$ hadron events and incoherent pairs, see presentation by E. Sicking

Readout and Power Pulsing

- Short luminous time (<200 ns) and long gap between trains (20 ms)
- Record data during collision time, read data out between trains
- *Triggerless* read out: all data are recorded
- When data is not being read out, switch off the detector: *Power Pulsing*

More in the presentations on *Vertex/tracker technologies* (D. Dannheim) and on *DAQ/readout considerations* (E. Sicking)

Very Forward Region

- Crossing angle of 20 mrad between beam axes
- Minimal acceptance of a cone of 10 mrad half-opening due to coherent pairs at 3 TeV
- Forward e.m. calorimeters: **LumiCal** and **BeamCal**, **ECal** and **HCal** endcaps
- The BeamCal is located in the centre of the HCal endcap

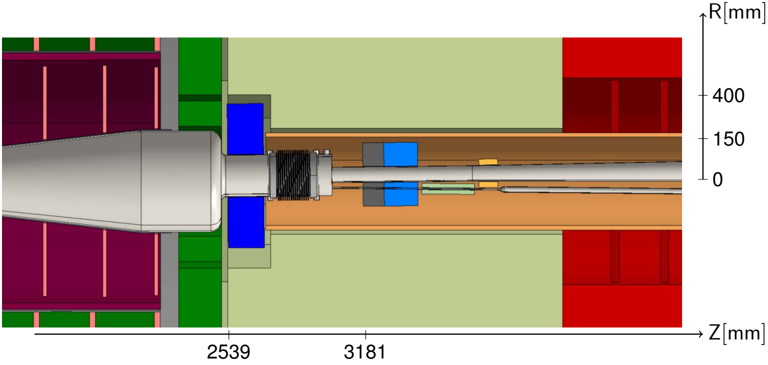

BeamCal and LumiCal

- The BeamCal (10–46 mrad) and LumiCal (39–134 mrad) are the most forward e.m. calorimeters
- BeamCal receives large energy deposits from incoherent pairs
  - Radiation dose: up to 1 MGy/yr and 10^{13} n_{eq}/yr/cm^{2} (at 3 TeV)
- LumiCal just outside the background envelope, suffers from backscattering particles
  - Precise polar angle and energy reconstruction for luminosity measurement

Deposited energy per pad from 40 BX of 3 TeV incoherent pairs in layer 9

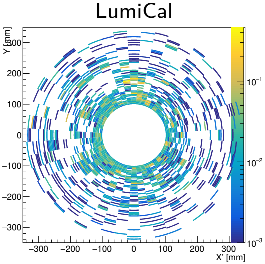

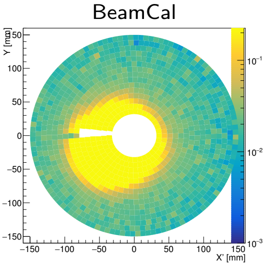

BeamCal and LumiCal

- The BeamCal (10–46 mrad) and LumiCal (39–134 mrad) are the most forward e.m. calorimeters
- BeamCal receives large energy deposits from incoherent pairs
  - Radiation dose: up to 1 MGy/yr and 10^{13} n_{eq}/yr/cm^2 (at 3 TeV)
- LumiCal just outside the background envelope, suffers from backscattering particles
  - Precise polar angle and energy reconstruction for luminosity measurement

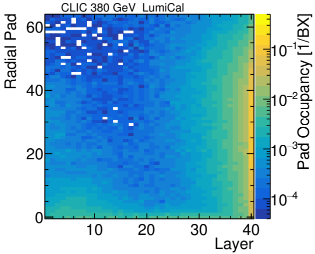

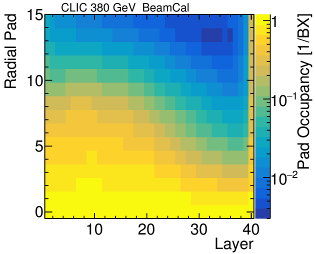

BeamCal and LumiCal

- The BeamCal (10–46 mrad) and LumiCal (39–134 mrad) are the most forward e.m. calorimeters
- BeamCal receives large energy deposits from incoherent pairs
  - Radiation dose: up to 1 MGy/yr and 10^{13} n_{eq}/yr/cm^2 (at 3 TeV)
- LumiCal just outside the background envelope, suffers from backscattering particles
  - Precise polar angle and energy reconstruction for luminosity measurement

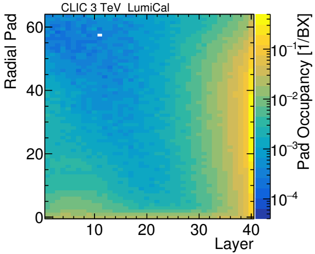

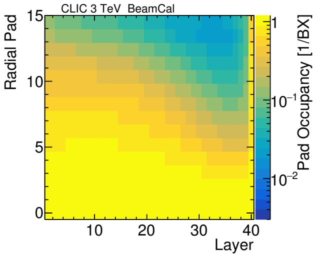

Calorimeter Endcaps

- The incoherent pairs showering in the BeamCal create a large neutron flux into the HCal endcap
- At the inner radius of the HCal endcap most cells see an energy deposit above 0.3 MIP per readout window

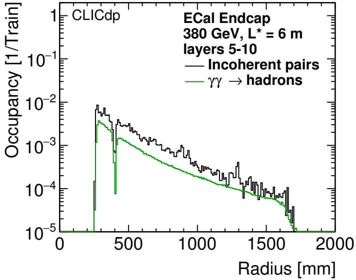

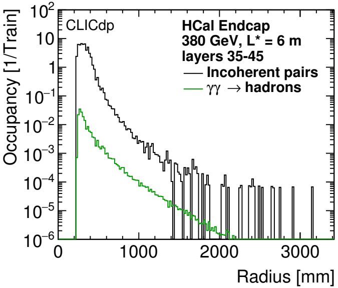

Calorimeter Endcaps

- The incoherent pairs showering in the BeamCal create a large neutron flux into the HCal endcap
- At the inner radius of the HCal endcap most cells see an energy deposit above 0.3 MIP per readout window

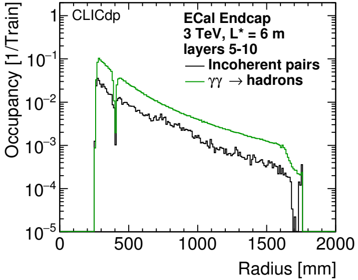

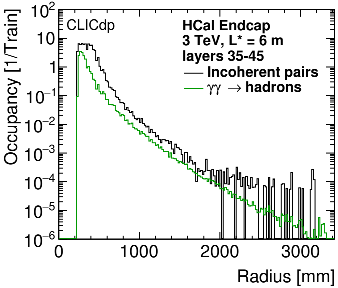

Calorimeter Endcaps

- The incoherent pairs showering in the BeamCal create a large neutron flux into the HCal endcap
- At the inner radius of the HCal endcap most cells see an energy deposit above 0.3 MIP per readout window
- Shielding inside the HCal endcap can absorb many of the particles and greatly reduce the occupancy, at the price of HCal endcap coverage [2]*

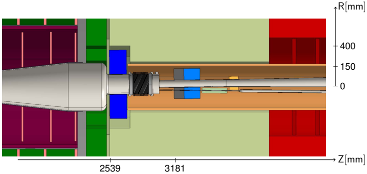

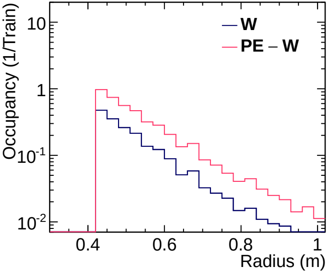

*Studies done with a previous detector model at 3 TeV

Calorimeter Endcaps

- The incoherent pairs showering in the BeamCal create a large neutron flux into the HCal endcap
- At the inner radius of the HCal endcap most cells see an energy deposit above 0.3 MIP per readout window
- Shielding inside the HCal endcap can absorb many of the particles and greatly reduce the occupancy, at the price of HCal endcap coverage [2]*
- Reducing the tile size also reduces the occupancy, at the price of higher number of channels [2]*

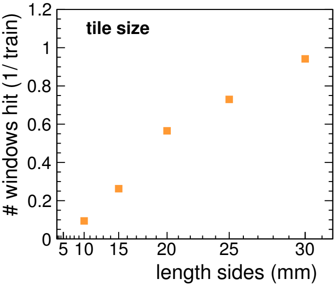

*Studies done with a previous detector model at 3 TeV

Section 3:

Background Mitigation Methods

Timing Cuts

Jet Clustering

Timing Cuts

- Read out full bunch train and identify time of physics event
- Select hits around the event using the time resolution of the sub-detectors
- Reconstruct objects: clusters and tracks
  - Calculate cluster time based on truncated mean time of hits, correct for time of flight
- Accept reconstructed particles depending on particle type, cluster time, and transverse momentum

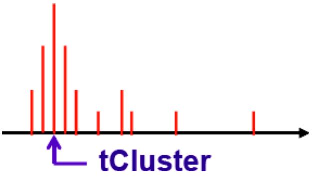

Default 3 TeV timing cuts

Region	p_T range	time cut
Photons		
central	$0.75\,\text{GeV} \leq p_T < 4.0\,\text{GeV}$	$t < 2.0\,\text{ns}$
$\cos\theta \leq 0.975$	$0\,\text{GeV} \leq p_T < 0.75\,\text{GeV}$	$t < 1.0\,\text{ns}$
forward	$0.75\,\text{GeV} \leq p_T < 4.0\,\text{GeV}$	$t < 2.0\,\text{ns}$
$\cos\theta > 0.975$	$0\,\text{GeV} \leq p_T < 0.75\,\text{GeV}$	$t < 1.0\,\text{ns}$
neutral hadrons		
central	$0.75\,\text{GeV} \leq p_T < 8.0\,\text{GeV}$	$t < 2.5\,\text{ns}$
$\cos\theta \leq 0.975$	$0\,\text{GeV} \leq p_T < 0.75\,\text{GeV}$	$t < 1.5\,\text{ns}$
forward	$0.75\,\text{GeV} \leq p_T < 8.0\,\text{GeV}$	$t < 2.0\,\text{ns}$
$\cos\theta > 0.975$	$0\,\text{GeV} \leq p_T < 0.75\,\text{GeV}$	$t < 1.0\,\text{ns}$
charged particles		
all	$0.75\,\text{GeV} \leq p_T < 4.0\,\text{GeV}$	$t < 3.0\,\text{ns}$
	$0\,\text{GeV} \leq p_T < 0.75\,\text{GeV}$	$t < 1.5\,\text{ns}$

Timing Cuts II

$e^{-}e^{+} \rightarrow HH$ with $\gamma\gamma \rightarrow$ hadron background overlaid before and after *tight* timing selection cuts

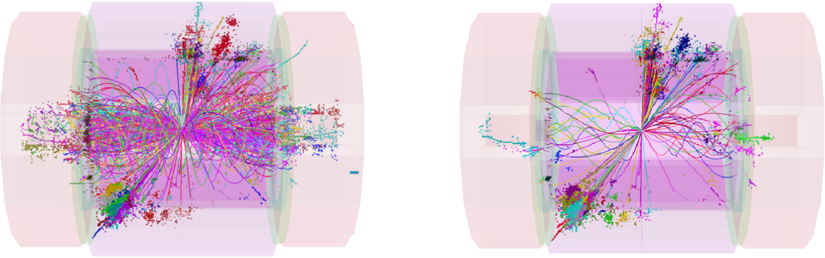

Jet Clustering

- $\gamma\gamma \to$ hadron background and longitudinal boost due to beamstrahlung make LEP jet algorithms unsuited for CLIC
- Use hadron collider jet algorithm features
  - Cluster forward particles into *beam* jets
  - Benefit from longitudinal invariance. Particle distance measure using $\Delta R^2 = \Delta\eta^2 + \Delta\phi^2$
- Specialised *VLC* jet algorithm [3]
- Reconstruction parameters can and have to be tuned to specific analyses, see the presentation on the physics studies

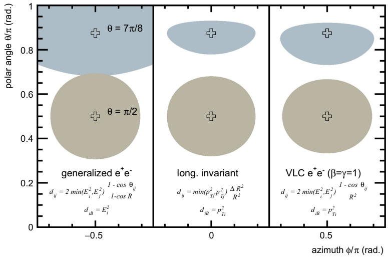

Jet areas obtained from different types of jet clustering algorithm

Section 4:

Luminosity Measurements

Absolute Luminosity Measurement
Luminosity Spectrum Reconstruction

Absolute Luminosity Measurement

- Absolute measurement of luminosity with Bhabha scattering gauge process
- Count number of events in very well defined polar and energy range $L = N/\sigma_{\text{Bhabha}}$
- LumiCal detector with excellent polar angle and energy resolution [1]
- Systematic effects from Beam-Beam effects under control [4]

Expected stat. uncertainty for 100 fb^{-1} at 3 TeV as a function of the minimal acceptance angle

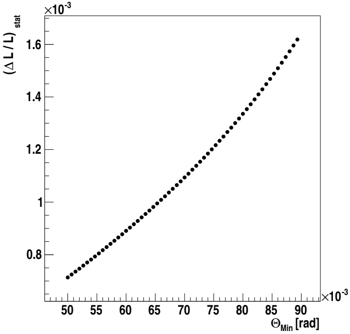

Luminosity Spectrum Reconstruction

- Reconstruct luminosity spectrum $\mathcal{L}(E_{e^-}, E_{e^+})$ from large angle ($\theta > 8^\circ$) Bhabha events
- 2D spectrum reconstruction at 3 TeV CLIC has been studied taking all relevant effects into account [5]

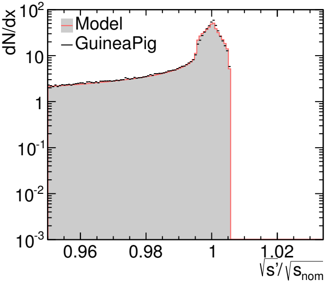

Simulated (Guinea-Pig) and reconstructed spectrum (model) after Bhabha scattering and detector resolutions

Section 5:

Summary

Summary

- High energy e^+e^- collisions are challenging, but still a lot cleaner than those of hadron machines
  - Worst case at $\sqrt{s} = 3$ TeV, a lot less background at $\sqrt{s} = 380$ GeV
- Combination of
  - detector time information,
  - granularity,
  - sophisticated reconstruction software: ConformalTracking, particle flow reconstruction,
  - jet clustering algorithms

  meet these challenges
- See next presentations for performance validation and physics performance

References

- H Abramowicz et al., "A Luminosity Calorimeter for CLIC", in: (Nov. 2009), URL: https://cds.cern.ch/record/1443828.
- S.B. van Dam and A. Sailer, "The occupancy in the Hadronic Calorimeter endcap of the CLIC detector", in: (2014), CLICdp-Note-2014-004.
- Ignacio Garcia Garcia et al., "Jet reconstruction at high-energy electron–positron colliders", in: *Eur. Phys. J. C* 78.2 (June 2017), p. 144.
- Strahinja Lukic, "Correction of beam-beam effects in luminosity measurement in the forward region at CLIC", in: (Jan. 2013), URL: https://cds.cern.ch/record/1507547.
- S. Poss and A. Sailer, "Luminosity Spectrum Reconstruction at Linear Colliders", in: *Eur. Phys. J. C* 74 (2014), p. 2833.

Backup Slides

Beam Parameters

Parameter	Unit	380 GeV	3 TeV
θ_c	mrad	16.5	20
f_{rep}	Hz	50	50
n_{b}		352	312
Δt	ns	0.5	0.5
N		$5.2 \cdot 10^9$	$3.72 \cdot 10^9$
σ_x	nm	≈ 149	≈ 45
σ_y	nm	≈ 2.9	≈ 1
σ_z	µm	70	44
β_x	mm	8	7
β_y	mm	0.1	0.12
L^*	m	6	6
$\mathcal{L}$	$1/\text{cm}^2\text{s}^1$	$1.5 \cdot 10^{34}$	$5.9 \cdot 10^{34}$
$\mathcal{L}_{0.01}$	$1/\text{cm}^2\text{s}^1$	$0.9 \cdot 10^{34}$	$2.0 \cdot 10^{34}$
n_γ		1.4	2.0
$\Delta E/E$		0.08	0.25
E_{coh}	TeV	≈ 0	$2.1 \cdot 10^8$
N_{coh}		≈ 0	$6.1 \cdot 10^8$
N_{incoh}		$4.6 \cdot 10^4$	$2.8 \cdot 10^5$
E_{incoh}	TeV	$2.1 \cdot 10^2$	$2.1 \cdot 10^4$
n_{Had} ($W_{\gamma\gamma} > 2$ GeV)		0.17	3.1

Beam Energy Position Correlation

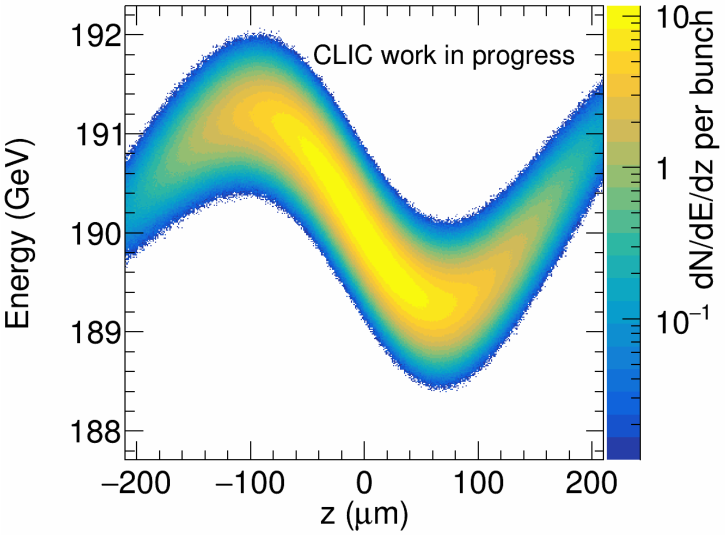

Beam Energyspread

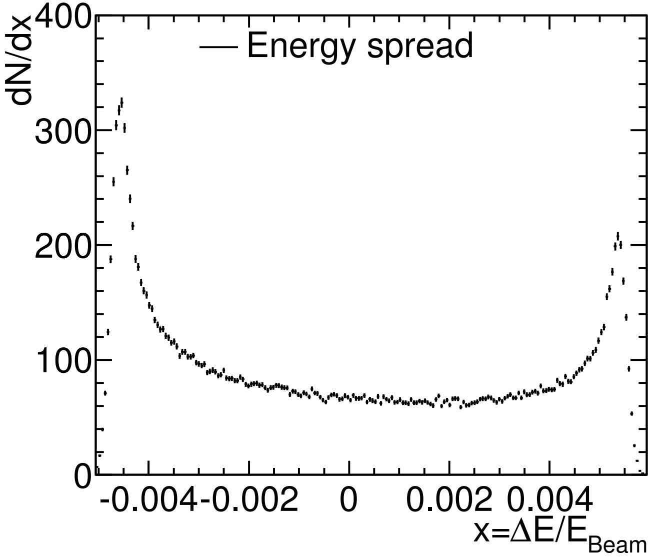

Spectrum Reconstruction in Two Slides

With the distribution $f(O_1, O_2, \ldots)$ of observables measurable in the Detector

$$f(O_1, O_2, \ldots) \approx \sigma(E_1, E_2; O_1, O_2, \ldots) \times \underline{\mathcal{L}\big(E_1, E_2\big)} \otimes \mathrm{ISR}\big(E_1, E_2\big) \otimes \mathrm{FSR}\big(O_1, O_2, \ldots\big) \otimes \mathrm{D}\big(O_1\big)\mathrm{D}\big(O_2\big) \ldots,$$

connected to the luminosity spectrum $\mathcal{L}\big(E_1, E_2\big)$ and measurable in the detector.
One can then:

- Model (i.e., parameterise) the luminosity spectrum
- Let Bhabha generator take care of cross-section and initial state radiation
- Do GEANT4 simulation for detector resolutions
- Use a reweighting technique for *efficient* fitting and extract $\mathcal{L}$

Reweighting Fit in Words

Reweighting technique uses χ^2-fit of two histogram with a distribution like

$$f(O_1, O_2, \ldots) \approx \sigma(E_1, E_2; O_1, O_2, \ldots) \times \underline{\mathcal{L}\left(E_1, E_2\right)} \otimes \mathrm{ISR}\left(E_1, E_2\right) \otimes$$
$$\mathrm{FSR}\left(O_1, O_2, \ldots\right) \otimes \mathrm{D}\left(O_1\right)\mathrm{D}\left(O_2\right) \ldots,$$

- Data histogram: measured in detector, spectrum simulated by GuineaPig, apply Bhabha-scattering and detector simulation
- MC histogram: Luminosity spectrum according to the Model, apply Bhabha-scattering and detector simulation
  - Apply Bhabha scattering/ISR/Detector resolutions on event-by-event basis via MC Generator and detector simulation
  - Remember initial probability based on luminosity spectrum of each event $\mathcal{L}\left(x_1^i, x_2^i; [p]_0\right)$
  - Vary all event probabilities (via Model parameters $[p]_N$) until minimum χ^2 is found

$$\text{event weight: } w^i = \frac{\mathcal{L}\left(x_1^i, x_2^i; [p]_N\right)}{\mathcal{L}\left(x_1^i, x_2^i; [p]_0\right)}$$

- Advantage
  - Only have to do (very time consuming) Bhabha-scattering and detector simulation once

Background Distribution